ЖУРНАЛ СТРУКТУРНОЙ ХИМИИ

2013. Том 54, № 2 *Март – апрель* *С. 228 – 236*

UDC 541.6:546.26:547.17

GAS-PHASE REACTION OF THE ISOBUTENYL ANION WITH N_2O FROM *AB INITIO* CALCULATIONS

J.X. Liang[1], Y.B. Wang[1], Z.Y. Geng[2], Y.Z. Wang[2], Y.C. Wang[2]

[1]*College of Chemical Engineering, Northwest University for Nationalities, Lanzhou, Gansu, P. R. China*
[2]*Gansu Key Laboratory of Polymer Materials, College of Chemistry and Chemical Engineering, Key Laboratory of Eco-environment-related Polymer Materials; Ministry of Education, Northwest Normal University, Lanzhou, Gansu, P. R. China*
E-mail: wangyb16@yahoo.cn

Received November, 23, 2011 *Revised — January, 8, 2012*

Calculations using conventional *ab initio* theory are performed to investigate the reaction mechanism associated with the gas-phase ion/molecule reaction of isobutenyl anion with N_2O. As a result, our theoretical findings strongly suggest that the main pathway is the reaction pattern of end-N attack and that the corresponding reaction mechanism basically relates to hydrogen migration, which may yield products *cis*-$CH_2(CH_3)CCN_2^-$, *trans*-$CH_2(CH_3)CCN_2^-$, and H_2O. Those are in good agreement with the experimental observations. Moreover, based on the NBO, Activation Strain model and methyl group effect analysis, we also explored the characters of rate-determining step of the main pathway.

K e y w o r d s: isobutenyl anion, reaction mechanism, second-order Møller—Plesset perturbation theory (MP2).

INTRODUCTION

Carbanion, acting as a sort of valuable electron-rich reagent, plays a central role in organic chemistry because of its widespread synthetic utility [1]. In many cases, it is a reactive nucleophilic intermediate [2—7] and is often encountered in organic chemistry, organometallic chemistry, alkyl lithium chemistry and so on [8—14]. Many experiments have demonstrated that the stable carbanions, owing to charge delocalization, do exist [2—15]. However, they have not been successfully isolated, possibly due to their high reactivities [9—11, 14]. Previously, substantial efforts were made to gain and characterize carbanions experimentally [12—14], including bond strengths, [16] energies, [17] and resonance effects. [18] Also, the corresponding gas-phase reactions have been studied extensively. [11—13, 19, 20] Here, the work of Depuy *et al.* in 1977 [19] in which, using a flowing afterglow (FA)-selected ion flow tube (SIFT), they investigated in detail the reaction mechanism of different carbanions with some small molecules, is most representative. Unfortunately, to the best of our knowledge, no theoretical study has hitherto well explored the reaction mechanism of an isobutenyl anion with N_2O, which was only inferred by Depuy from the experiment [20], as shown in Scheme 1.

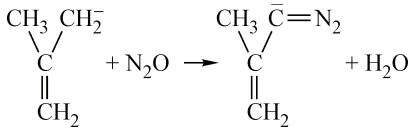

Scheme 1

Therefore, we are strongly stimulated to carry out the work to elucidate the mechanism of this reaction and to give a suitable explanation for the experimental results. Furthermore, through this theoretical work, we hope (i) to estimate the crucial activation barriers and to understand the origin of the barrier heights using the Activation Strain model, and (ii) to investigate the methyl group effect on the preferred reaction pathways.

COMPUTATIONAL METHODS

All calculations were carried out using the Gaussian 03 program [21]. For the reaction of the isobutenyl anion with N_2O, the geometries of the reactants, the products, the intermediate isomers and the transition states were fully optimized at the MP2/6-31++G(*d*,*p*) level [22]. Frequency calculations at the same level of theory have been performed to identify all of the stationary points as minima (zero imaginary frequency) or transition-state structures (one imaginary frequency). The relative energies were, thus, corrected for vibrational zero-point energies (ZPE) and the transition states both to the reactant and the product directions in the reaction pathways were examined by the intrinsic reaction coordinate (IRC) [23]. To obtain more reliable energetic data, higher-level single-point energy calculations were performed at the QCISD [24] level of theory with the same basis set (QCISD/6-31++G(*d*,*p*)) using the MP2/6-31++G(*d*,*p*) optimized geometries. Moreover, the natural population analysis (NPA) has been conducted with the natural bond orbital (NBO) method [25].

RESULTS AND DISCUSSION

Figs. 1, 2 and 3 show the equilibrium geometries for the title reaction obtained by the optimization procedure at the MP2 theory level using 6-31++G(*d*,*p*) basis set, where the computed structures are labeled as IM or TS depending on their nature as intermediates or transition states. The energy profiles obtained at the QCISD/6-31++G(*d*,*p*)//MP2/6-31++G(*d*,*p*) level are depicted in Fig. 4. The more detailed information will be discussed in the following sections.

Entrance channels. Our calculations show that a weakly bonded van der Waals complex named IM1 is formed firstly for the title reaction when isobutenyl anion approaches an N_2O molecule. This is fully consistent with the predictions [12—14, 19, 20]. As illustrated in Fig. 1, IM1 is very reactant-like and more stable than the reactant asymptote by 29.25 kJ/mol. Therefore, the formation of IM1 will provide enough exothermic energy to activate itself, resulting in the reaction continuing until the formation of different products. Note that the C^1 and C^3 in IM1 can be considered as the most active sites, which is supported by the largest negative charge concentration found at the two symmetric C^1 and C^3 atoms, cal. the same –0.847 a.u. (Scheme 2). Here, the active site is limited to the C^1 in the present study. Starting from IM1, the association with N_2O may have three attack patterns, that is, (i) end-O attack to form IM2-O; (ii) middle-N attack to form IM2′; (iii) end-N attack to form IM2. This is consistent with the experimental results proposed by Depuy *et al*., [26] who found that N_2O was capable of donating one or two nitrogen atoms or an oxygen atom. In addition, according to the molecular orbital (MO) theory [27—29], the difference in stability of the molecule is easily understood in terms of the HOMO(Lewis base)—LUMO(Lewis acid) interaction, namely, both a smaller HOMO—LUMO gap (ΔE) facilitates the electron transition in general, but is unfavorable for the formation of a Lewis steady molecule. Our theoretical result indicates that the corresponding ΔE of the three molecules fall in the order IM2-O (756.14) > IM2 (732.52) > IM2′ (685.26), as shown in Table 1. This is fully confirmed by our theoretical calculations. As shown in Fig. 4, the relative energies with reference to R ($C_4H_7^- + N_2O$) for the three complexes obtained at the QCISD/6-31++G(*d*,*p*)//MP2/6-31++G(*d*,*p*) level are –85.98 kJ/mol (IM2′), –182.24 kJ/mol (IM2) and –371.07 kJ/mol (IM2-O), respectively. Consequently, it is reasonable that the stabilization of the complexes exhibits an increasing trend as IM2-O > IM2 > IM2′. However, as shown in Fig. 4, the further evolution

Table 1

Molecular orbital energies (kJ)

	IM2	IM2′	IM2—O
HOMO	–385.95	–333.44	–378.07
LUMO	346.57	351.82	378.07
$\Delta E = E_{LUMO} - E_{HOMO}$	732.52	685.26	756.14

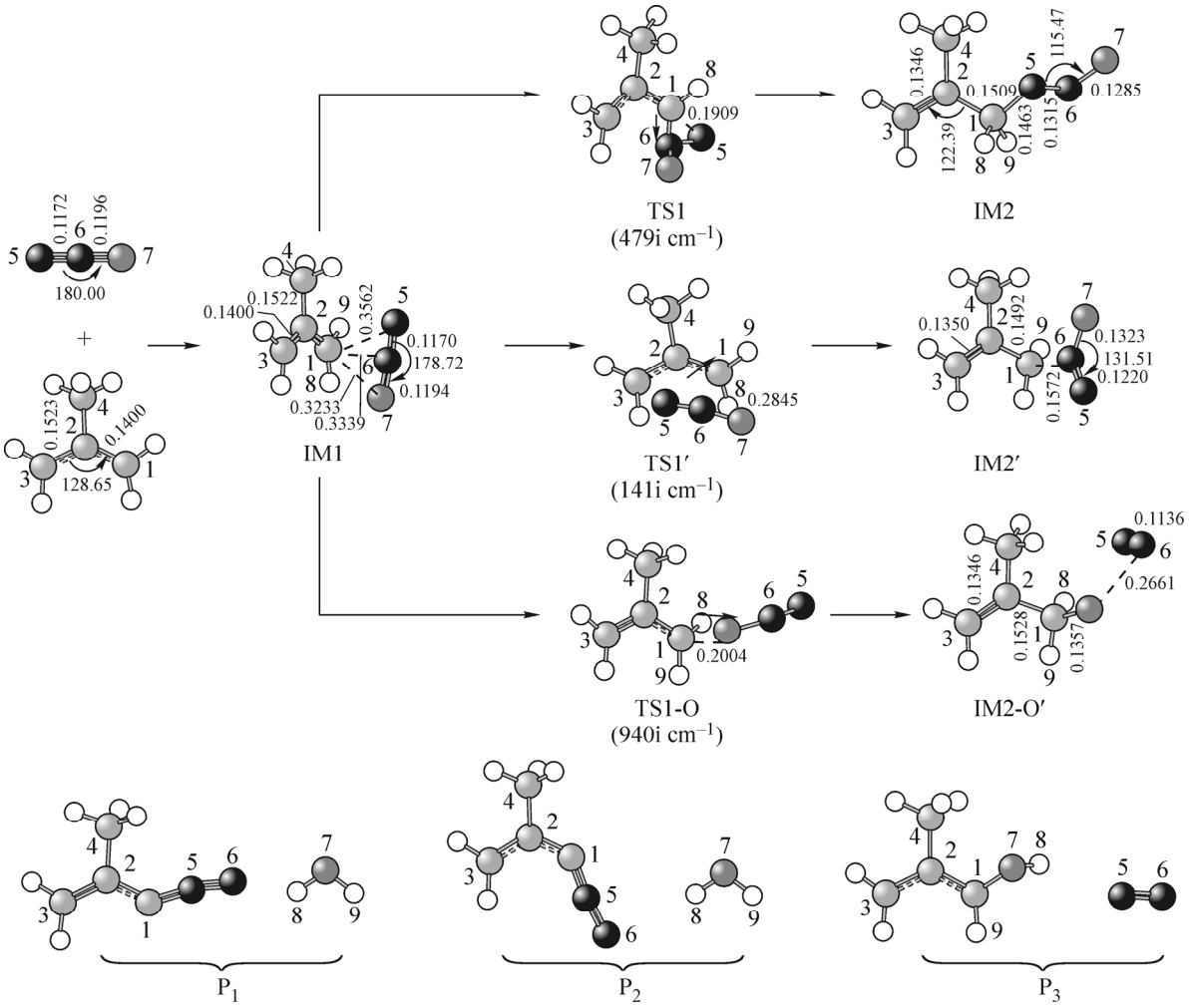

Fig. 1. Optimized geometries of all the reactants, the products and the initial step of reaction of isobutenyl anion with N_2O at the MP2/6-31++G(*d*,*p*) level of theory. Bond distances in nm and angles in degree

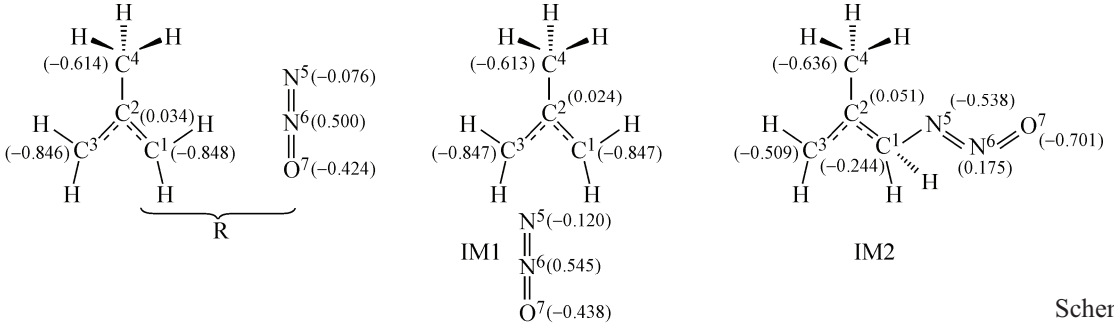

Scheme 2

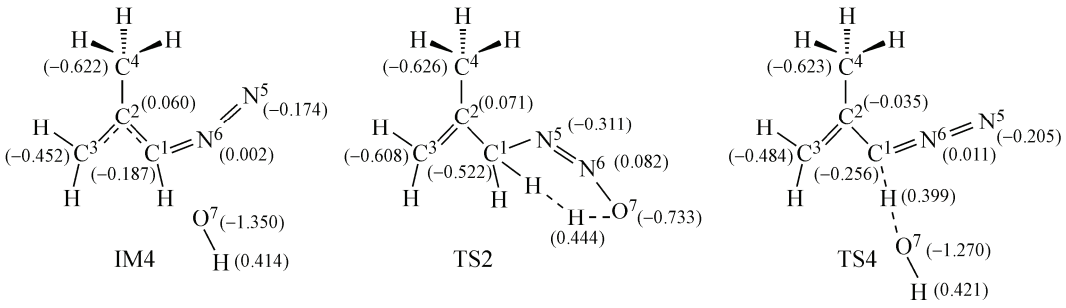

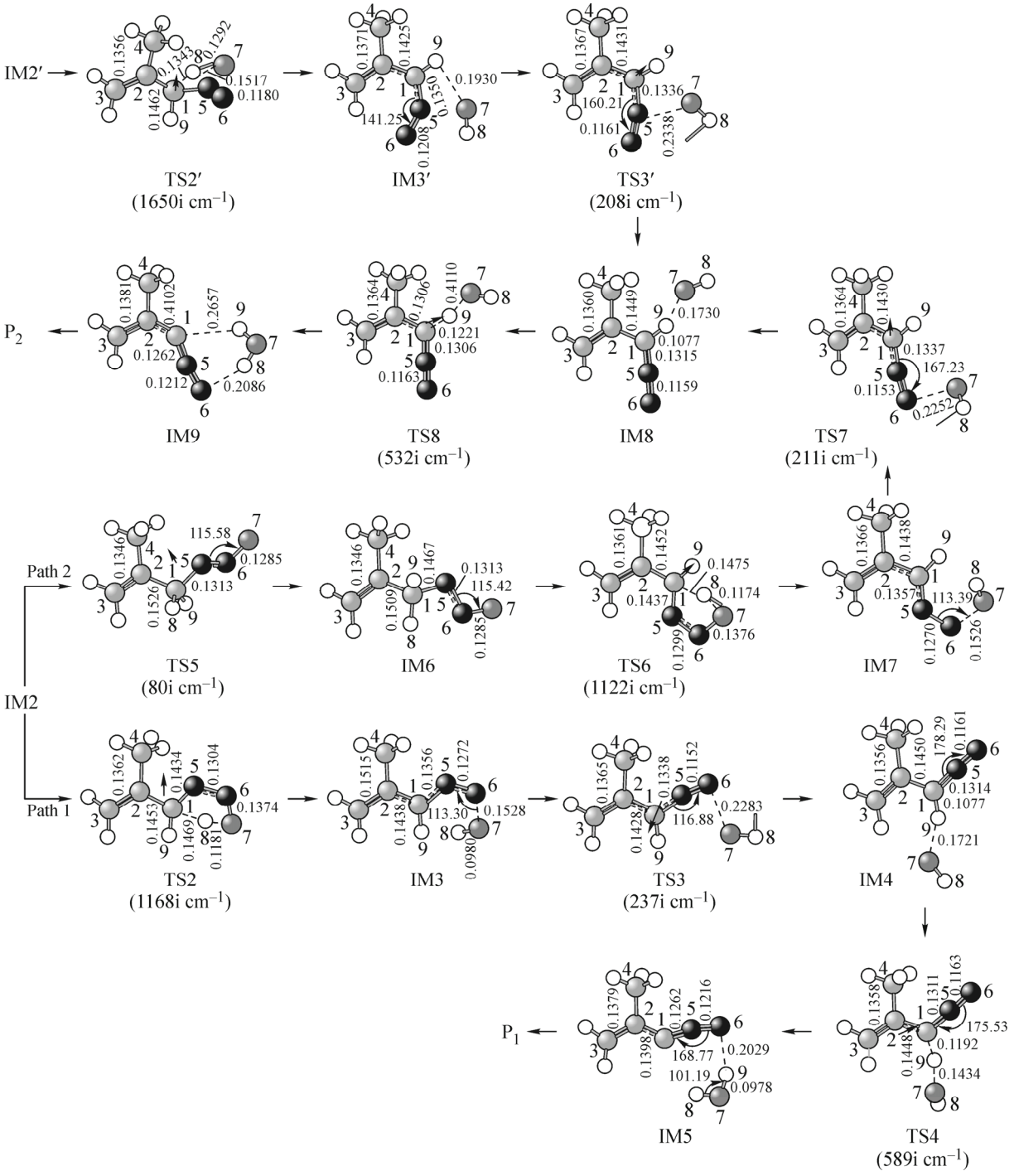

Fig. 2. Optimized geometries of all the isomers and transition states for the reaction isobutenyl anion+N_2O at the MP2/6-31++G(*d*,*p*) level of theory. Bond distances in nm and angles in degree

pathway of IM2′ (IM2′ → TS2′ → IM3′) involves a high-energy transition state TS2′ (68.04), which indicates that these processes may be not at all preferred in energy and have little contribution to the final products. It is certainly consistent with experimental results [30, 31] which propose that the initial nucleophilic attack generally occurs at the terminal nitrogen atom, but does not rule out the attack at the central nitrogen atom. By comparison, in the formation of IM2-O (IM1 → TS1-O → IM2-O) the relative energy of the rate-determining transition state TS1-O lies (18.81) somewhat higher than that

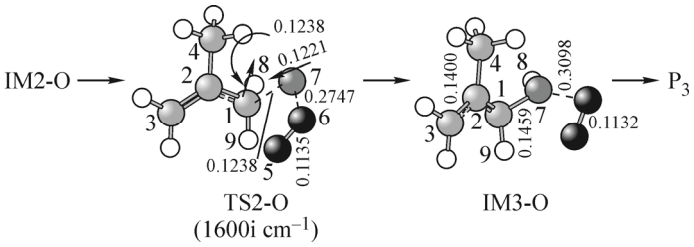

Fig. 3. Optimized geometries of the O-atom direct abstraction reaction of isobutenyl anion with N_2O at the MP2/6-31++G(*d*,*p*) level of theory. Bond distances in nm and angles in degree

of the reactants, and the step is strongly exothermic by 371.07 kJ/mol. Thus, on the whole, the pathway is more preferable thermodynamically, but is kinetically less likely. However, we have failed to try to locate the other channel that assumed the reaction channel: $(H_7C_4)^- + N_2O \rightarrow (H_2C{=}C{-}CH_3)^- + N_2 + H_2C{=}O$ [19]. Presumably this is due to the methyl group effect that contributes to the C^2—C^1 bond of the isobutenyl anion, making it shorter so to be unfavorable towards the loss of formaldehyde. As a result, our investigation indicated that the reaction from IM3-O proceeded through only α-H migration to yield separated products $[C_4H_6OH]^- + N_2$, rather than via the C^1—C^2 breakage to produce $H_2C{=}O$, as shown in Fig. 3. Thus, in the following passage, we concentrate on the isomers of IM2 and its subsequent evolution.

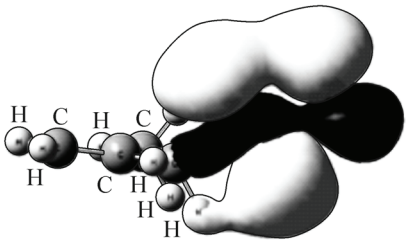

Scheme 3. Sketch of the orbital interaction at the intermidiates IM2

Nature of IM2. It can be seen from Fig. 1 that in IM2 the covalent bond C—N $(0.6597(sp^{3.03}d^{0.01})_C + 0.7515(sp^{2.50}d^{0.01})_N)$ formed between the isobutenyl anion and the N_2O molecule can be rationalized considering the donation of electron density from the lone pair of C (isobutenyl anion) electrons into empty 2*p* orbitals of N_2O. As shown in Scheme 3, *a* σ—π* orbital interaction occurs between C^1 of the isobutylene anion and N^5 of N_2O which leads to the hybridization state of N^5 changing to sp^2 from sp. This interaction also reflects that the observably changed structures appear to the N_2O group due to the weakening of the conjugated π bond. For instance, the N—N—O bond angle is diminished from 178.72° to 115.47°, with an increase of 0.0143 nm in the N—N bond and 0.0089 nm in the N—O bond compared to the isolated N—N (0.1172 nm) and N—O (0.1196 nm) bonds of free N_2O. The NBO analysis indicates there is a net electronic transfer of 1.064 a.u. (Scheme 2) from the isobutenyl moiety to the N_2O fragment. For the formation of IM2, as displayed in Fig. 4, from IM1 it is necessary to surmount an activation barrier of 18.81 kJ/mol via TS1 (479i cm^{-1}) with 10.44 kJ/mol lower than the separated reactants. Consequently, the step of IM1 → IM2 may proceed much more easily on the PES. Presumably this is due to the effect of the methyl group which contributes to α-C activated.

Isomerization and dissociation. Starting from the IM2 isomer (–182.24), the reaction bifurcates into two equivalent uphill pathways to reach TS2 and TS5, respectively. One named pathway **(1)** is the H^8 attached to the C^1 transfer to the O^7 to form hydroxide ion OH^-, followed by concerted OH^--abstract to α-H^9 along with H_2O-extrusion to generate P_1 (*trans*-$CH_2(CH_3)CCN_2^-$ + H_2O) (–102.27). The other named pathway **2** is the concerted conversion of IM2 to its structural isomer IM6 (–178.85) along with the subsequent reaction mechanism same as pathway **1** to yield P_2 (*cis*-$CH_2(CH_3)CCN_2^-$ + H_2O) (–105.74). Generally, the energy barrier controls the reaction rate in a pathway. Thus, we use barrier height to discuss the feasibility of pathways **1** and **2**. Considering the rather close barriers, 112.93 (IM2 → TS2 → IM3) kJ/mol in pathway **1** and 109.34 (IM6 → TS6 →

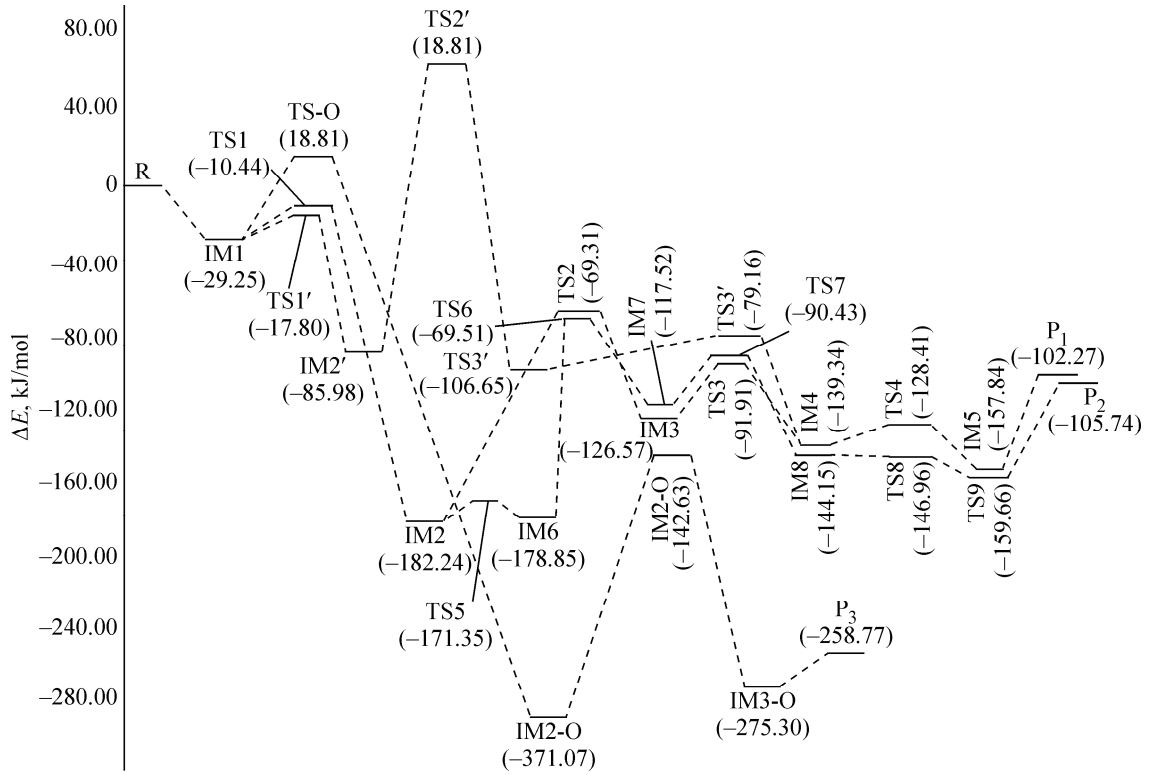

Fig. 4. Singlet potential energy (kJ/mol) surface of all the reaction channels for the reaction of isobutenyl anion with N_2O at the QCISD/6-31++G(*d*,*p*)//MP2/6-31++G(*d*,*p*) level of theory

→ IM7) kJ/mol in pathway **2**, formation of P_1 (*trans*-$CH_2(CH_3)CCN_2^-$ + H_2O) and P_2 (*cis*-$CH_2(CH_3)CCN_2^-$ + H_2O) is quite competitive. As a consequence, reflected in the final product distributions, *trans*-$CH_2(CH_3)CCN_2^-$, *cis*-$CH_2(CH_3)CCN_2^-$ and H_2O may be the most favorable products. In the following discussion, we will only explain in detail pathway **1**.

Pathway 1. As shown in Fig. 2, pathway **1** can overall be written as: IM2 → TS2 → IM3 → → TS3 → IM4 → TS4 → IM5 → P_1. Our calculations show that a hydrogen migration from C^1 to O^7, via an intramolecular proton-transfer process, is the first stage (IM2 → IM3) forming IM3. The corresponding transition structure TS2 presents one imaginary frequency of 1168i cm^{-1} and the H^8 (attached to the C^1 atom) being transferred carries a negative charge of 0.102 a.u. As displayed in Fig. 2, the labeled transition vector clearly corresponds to the expected movement of H^8 detaching from C^1 and moving towards O^7. As shown in Fig. 4, the step is a very steep process, namely, from IM2 it is necessary to surmount an activation barrier of 112.93 kJ/mol to reach TS2 and then go down to IM3, which is 126.57 kJ/mol more stable than the separated reactants. The second step (IM3 → IM4) involves the loss of a hydroxide ion and at the same time IM4 is formed via the transition state TS3, characterized by an imaginary frequency of 237i cm^{-1} and situated 91.91 kJ/mol below the reactant asymptote. The transition vector for the imaginary frequency, also labeled in Fig. 2, clearly indicates the OH^- transfer, which helps the sequent reaction (hydrogen transfer) occur. The NBO analysis (Scheme 2) shows that the negative charge on the HO unit in IM4 is –0.936 a.u. As such, the resulting $C_4H_6N_2$—OH^- complex is best described as an ion dipole complex between the OH^- and molecular $C_4H_6N_2$ (Fig. 2). Note that IM4 is more stable than IM3 by 12.77 kJ/mol as displayed in Fig. 4. Presumably this is due to that minimum IM4 lives longer while OH^- searches for a suitable hydrogen proton to undergo abstraction. The third step (IM4 → IM5) is the second α-H^9 abstract reaction via the transition state TS4 (only one imaginary frequency 589i cm^{-1}) to yield an adduct IM5. In IM5, the H_2O unit of the complex is virtually identical to the separated molecular H_2O, where the O—H distances (0.9782 nm) and H—O—H

Table 2

Activation strain analysis of the activation barriers [a]

	$\Delta E^{\neq}$	$\Delta E^{\neq}_{\text{strain}}$	$\Delta E^{\neq}_{\text{int}}$
TS2	112.93	939.48	–826.55
TS4	10.93	335.84	–324.91
TS2/TS4 (ratio)	10.34	2.80	2.54

[a] Values are reported in kJ/mol at the QCISD//MP2.

bond angles (101.19°) are nearly the same compared with those of the calculated equilibrium bond lengths and bond angles of molecular H_2O (0.9600 nm and 109.50°). Finally, from the product-like complex IM5, the separated products *trans*-$CH_2(CH_3)CCN_2^- + H_2O$, can be directly obtained surmounting a higher barrier height of 57.57 kJ/mol. As shown in Fig. 4, the PES is very flat in the exit channel.

As shown in Fig. 2, along pathway **1** the stepwise hydrogen abstract reaction passes through three transition states (TS2, TS3 and TS4) to render *trans*-$CH_2(CH_3)CCN_2^- + H_2O$ and the total reaction energy is 102.27 kJ/mol exothermic. It must be noted that the activation energy of the first hydrogen abstract (from IM2 to IM3, Fig. 4) exceeds that (from IM4 to IM5, Fig. 4) of the second hydrogen abstract by 102.00 kJ/mol. Thus, the second abstraction reaches the TS relatively rapidly compared to the first abstraction which arrives at the TS relatively slowly. According to the Hammond postulate [32], TS4 has stronger reactant-like character than TS2. This was fully confirmed by our theoretical calculations. As shown in Fig. 4, the step of IM2 → IM3 is predicted to undergo an endothermic abstraction whereas the step of IM4 → IM5 is an exothermic process. Moreover, we have analyzed the nature of crucial activation barriers of the elementary steps (IM2 → IM3 and IM4 → IM5, Fig. 4) using the Activation Strain model [33—36] in which the activation energy $\Delta E^{\neq}$ is decomposed into the activation strain $\Delta E^{\neq}_{\text{strain}}$ and the stabilization transition state (TS) interaction $\Delta E^{\neq}_{\text{int}}$ between the reactants in the activated complex: $\Delta E^{\neq} = \Delta E^{\neq}_{\text{strain}} + \Delta E^{\neq}_{\text{int}}$. In the paper, the activation strain $\Delta E^{\neq}_{\text{strain}}$ refers to the relative energy of the total energy of the deformed reactants (isobutenyl and N_2O moieties in TS2 and $C_4H_6N_2$ and OH segments in TS4, respectively) in the geometry of activated complex with that of IM2 and IM4. The transition state interaction $\Delta E^{\neq}_{\text{int}}$ is the relative energy of the total energy of the deformed reactants with that of the corresponding TS. As shown in Table 2, comparison of the $\Delta E^{\neq}_{\text{strain}}$ and $\Delta E^{\neq}_{\text{int}}$ components in TS2 and TS4 reveals that the $\Delta E^{\neq}_{\text{strain}}(\text{TS2})/\Delta E^{\neq}_{\text{strain}}(\text{TS4})$ is 2.80, but the $\Delta E^{\neq}_{\text{int}}(\text{TS2})/\Delta E^{\neq}_{\text{int}}(\text{TS4})$ is 2.54 and the net result is the $\Delta E^{\neq}(\text{TS2})/\Delta E^{\neq}(\text{TS4})$ is 10.34. Obviously, $\Delta E^{\neq}_{\text{strain}}$ is a major factor determining activation energy. The quantitative analysis has provided evidence to better demonstrate that the step of the second hydrogen abstraction is preferable in energy than that of the first hydrogen abstraction.

In order to understand the competition between the two hydrogen abstraction steps in detail, for IM2 → IM3 and IM4 → IM5, second-order perturbation analyses and principal delocalizations were carried out for all possible interactions between the filled Lewis-type NBOs and the empty non-Lewis NBOs. According to NBO analysis, for TS4 the large stabilization energies of $\sigma(C^1—H^9) \rightarrow \sigma^*(N^5—N^6)$ (68.03) and LP $(O^7) \rightarrow \sigma^*(C^1—H^9)$ (437.77) indicate that the dominant hyperconjugative effects make the energy of TS4 lower, which makes the hydrogen transfer between C^1 and O^7 facile. Comparatively, the small stabilization energies for TS2 ($\sigma(C^1—H^8) \rightarrow \sigma^*(N^5—N^6)$ (66.53) and LP $(O^7) \rightarrow$ $\rightarrow \sigma^*(C^1—H^8)$ (68.83)) indicate that the dominant hyperconjugative interaction exists in the TS2 system, which hinders the $O^7—H^8$ interaction and makes the formation of IM3 rather difficult. Additionally, as shown in Scheme 2, the electron density difference between C^1 and O^7 of TS2 is smaller than that of TS4 (0.211 a.u. for TS2 and 1.014 a.u. for TS4), which helps the hydrogen transfer in TS4. Therefore, the step of the second hydrogen abstraction is very important to make the reaction proceed.

Pathway 2. As shown in Fig. 2, pathway **2** can be expressed overall as follows: IM2 → TS5 → → IM6 → TS6 → IM7 → TS7 → IM8 → TS8 → IM9 → P_2. Starting from IM6 derived from the isomerization of IM2, the reaction pathway yielded P_2 (cis—$CH_2(CH_3)CCN_2^- + H_2O$) which is completely identical with pathway **1** described above. It should be noted that, as shown in Fig. 4, the energies of the transition states TS6 (–69.51 kJ/mol), TS7 (–90.43 kJ/mol) and TS8 (–146.96 kJ/mol) in

this pathway are all lower than that of the reactant asymptote. Therefore, starting from IM2, it is very significant to make the reaction proceed along pathway **2**.

Methyl group effect analysis. To better understand the reaction of the isobutenyl anion with N_2O, we have recalled an analogous reaction, allyl anion + N_2O [37, 38]. By comparison, the apparent discrepancy for the two types of reactions lies in rate-determining steps (reflecting on the first α-H migration) of their main pathways, that is, the isobutenyl anion reaction was estimated by a higher barrier in the step, as compared to the allyl anion reaction. Presumably this is mainly due to the existence of methyl group which, exhibiting better electron-donation ability, contributes to the α-C—H bond of the isobutenyl anion, which is due to an increase in negative charge on α-C atom, is unfavorable towards H-atom migration. This methyl group effect is also reflected in the fact that the former formation of the hydroxide ion and the latter second α-H abstraction are not concerted in the isobutenyl anion reaction as compared to the allyl anion reaction with concerted characters, which is well consistent with the result obtained by Ichino *et al.* [38] who found that the corresponding processes probably encountered a small energy barrier along the reaction pathway. As a prediction, although we have not carried out those calculations for the methyl group of the isobutenyl anion substituted by halogen reactions using the same level of theory in this work, a similar phenomenon can be found: the second α-H migration is the rate-determining step and the second α-H migration and OH dissociation may be concerted due to halogen characters. It is hoped that our study will stimulate further research into the subject.

CONCLUSIONS

To gain further insight into the reaction mechanism of the isobutenyl anion with N_2O in the gas phase, a detailed theoretical investigation on PESs has been performed with quantum chemical methods. The theoretical data obtained may provide a helpful tool for the interpretation of experimental observation and a useful guide for understanding the mechanism of other analogous reactions. The conclusions of the present study can be summarized as follows: (1) the formation of the initial encounter complex is spontaneous and it is a barrierless process, when the isobutenyl anion approaches N_2O; (2) the main pathways expressed as pathways **1** and **2**, which are two reciprocally competitive pathways, are reaction patterns of end—N attack. This is in agreement with the experimental result. Pathway **1** proceeds via a three-step manner mostly involving hydrogen transfer to yield products P_1 (*trans*-$CH_2(CH_3)CCN_2^-$ + H_2O), and in pathway **2**, after the isomerization of IM2 to IM6, a similar pathway 1 mechanism is traced to form products P_2 (*cis*-$CH_2(CH_3)CCN_2^-$ + H_2O); (3) using the Activation Strain model analysis, it is inferred that $\Delta E_{\text{int}}^{\neq}$ cannot dominate the activation barriers of the title reaction; (4) based on our investigation in this paper, the methyl group effect may change conventional mechanisms and influence the rate-determining step in the reactions.

Project is supported by the Northwest University for Nationalities (No. xbmuyjrc201107) and The Fundamental Research Funds for the Central Universities (No. zyz2011059).

REFERENCES

1. *Depuy C.H.* // Int. J. Mass. Spectrom. – 2000. – **200**. – P. 79 – 96.
2. *Carey F.A., Sundberg R.J.* Advanced organic chemistry, Part A: structure and mechanisms, 2nd ed., Plenum Press, New York, 1984.
3. *March J.* Advanced organic chemistry: reactions, mechanisms and structure, 3rd ed., Wiley, New York, 1985.
4. *Gilchrist T.C., Rees C.W.* Carbenes, nitrenes and arynes, Nelson, London, 1969.
5. *Bug T., Lemek T., Mayr H.* // J. Org. Chem. – 2004. – **69**. – P. 7565 – 7576.
6. *Ofial A.R., Mayr H.* // Macromol. Symp. – 2004. – **215**. – P. 353 – 367.
7. *Lucius R., Loos R., Mayr H.* // Angew. Chem. – 2002. – **114**. – P. 97 – 102. // Angew. Chem. Int. Ed. – 2002. – **41**. – P. 91 – 95.
8. *Wu G., Huang M.* // Chem. Rev. – 2006. – **106**. – P. 2596 – 2616.
9. *Walton J.C., Marshall L.J., Roydhouse M.D., Slawin A.M.Z.* // J. Org. Chem. – 2007. – **72**. – P. 898 – 911.

10. *Richey H.G.* Grignard reagents: new developments, Wiley, New York, 2000.
11. *Maruyama K., Katagiri T.* // J. Phys. Org. Chem. – 1989. – **2**. – P. 205 – 213.
12. *Applequist D.E., Peterson A.H.* // J. Amer. Chem. Soc. – 1961. – **83**. – P. 862 – 865.
13. *Kapeller D., Barth R., Mereiter K., Hammerschmidt F.* // J. Amer. Chem. Soc. – 2007. – **129**. – P. 914 – 923.
14. *Nobe Y., Arayama K., Urabe H.* // J. Amer. Chem. Soc. – 2005. – **127**. – P. 18006 – 18007.
15. *Olmstead M.M., Power P.P.* // J. Amer. Chem. Soc. – 1985. – **107**. – P. 2174 – 2175.
16. *Ervin K.M., Gronert S., Barlow S.E., Giles M.K., Harrison A.G., Bierbaum V.M., DePuy C.H., Lineberger W.C., Ellison G.B.* // J. Amer. Chem. Soc. – 1990. – **112**. – P. 5750 – 5759.
17. *Jordan K.D., Burrow P.D.* // Chem. Rev. – 1987. – **87**. – P. 557 – 588.
18. *Bartmess J.E., McIver R.T., Bowers M.T.* In gas phase ion chemistry; Ed.; Academic Press: New York, 1979.
19. *Bierbaum V.M., Depuy C.H., Shapiro R.H.* // J. Amer. Chem. Soc. – 1977. – **99**. – P. 5800 – 5802.
20. *Kass S.R., Filley J.J., Doren M.V., Depuy C.H.* // J. Amer. Chem. Soc. – 1986. – **108**. – P. 2849 – 2852.
21. *Frisch M.J., Trucks G.W., Schlegel H.B. et al.* Gaussian 03, Revision B. 01. Pittsburgh, PA: Gaussian Inc., 2003.
22. *Hehre W.J., Radom L., Schleyer P.v.R., Pople J.A. Ab initio* molecular orbital theory, John Willey & Sons, New York, 1986.
23. *Fukui K.* // Acc. Chem. Res. – 1981. – **14**. – P. 363 – 368.
24. *Pople J.A., Head-Gordon M., Raghavachari K.* // J. Chem. Phys. – 1987. – **87**. – P. 5968 – 5916.
25. *Reed A.E., Weinhold L.A.F.* // Chem. Rev. – 1988. – **88**. – P. 899 – 926.
26. *O'Hair R.A., Gronert S., DePuy C.H.* // Eur. Mass. Spectrom. – 1995. – **1**. – P. 429 – 436.
27. *Moss R.A., Fedorynski M., Shieh W.C.* // J. Amer. Chem. Soc. – 1979. – **101**. – P. 4736 – 4738.
28. *Smith N.P., Stevens I.D.R.* // J. Chem. Soc., Perkin. Trans. 2. – 1979. – P. 1298 – 1308.
29. *Moss R.A.* // Acc. Chem. Res. – 1980. – **13**. – P. 58 – 64.
30. *Dawson J.H.J., Nibbering N.M.M.* // J. Amer. Chem. Soc. – 1978. – **100**. – P. 1928 – 1929.
31. *Barlow S.E., Bierbaum V.M.* // J. Chem. Phys. – 1990. – **92**. – P. 3442 – 3448.
32. *Hammond G.S.* // J. Amer. Chem. Soc. – 1955. – **77**. – P. 334 – 338.
33. *Blowers P., Ford L., Masel R.* // J. Phys. Chem. A. – 1998. – **102**. – P. 9267 – 9277.
34. *Diefenbach A., Bickelhaupt F.M.* // J. Chem. Phys. – 2001. – **115**. – P. 4030 – 4040.
35. *Diefenbach A., de Jong G.T., Bickelhaupt F.M.* // J. Chem. Theory. Comput. – 2005. – **1**. – P. 286 – 298.
36. *de Jong G.T., Bickelhaupt F.M.* // J. Chem. Theory. Comput. – 2007. – **3**. – P. 514 – 529.
37. *Liu L.-Y., Geng Z.-Y., Zhao C.-Y., Wang Y.-C., Li Z.-H.* // Acta. Phys. Chim. Sinica. – 2007. – **2**. – P. 217 – 222.
38. *Ichino T., Gianola A.J., Kato S., Bierbaum V.M., Lineberger W.C.* // J. Phys. Chem. A. – 2007. – **111**. – P. 8374 – 8383.